Research Square

Preprints are preliminary reports that have not undergone peer review.
They should not be considered conclusive, used to inform clinical practice,
or referenced by the media as validated information.

Reducing Energy Storage Requirements in Renewable Mini-grids through Hybridization

Asmelash Haftu Amaha

asmelashx@gmail.com

Indian Institute of Technology Bombay https://orcid.org/0000-0001-7877-5883

Anand B. Rao

a.b.rao@iitb.ac.in

Indian Institute of Technology Bombay

Research Article

Keywords: Hybrid renewable energy systems, Renewable mini-grids, Battery energy storage, Material efficiency, Rural electrification, Techno-economic assessment, HOMER Pro, Hybridization

Posted Date: May 28th, 2026

DOI: https://doi.org/10.21203/rs.3.rs-9818671/v1

License: This work is licensed under a Creative Commons Attribution 4.0 International License.
Read Full License

Additional Declarations: The authors declare no competing interests.

Reducing Energy Storage Requirements in Renewable Mini-grids through Hybridization

Asmelash Haftu Amaha[1,], Anand B. Rao[1]

Centre for Technology Alternatives for Rural Areas (C-TARA)
Indian Institute of Technology Bombay, Powai 400076, India
asmelashx@gmail.com, a.b.rao@iitb.ac.in

Abstract

Comparative assessment of hybrid renewable energy systems (HRES) is critical for identifying cost-effective and storage-efficient mini-grid configurations. Battery energy storage remains one of the dominant cost and material burdens in off-grid renewable mini-grids, particularly in solar-only systems. This study demonstrates that storage requirements can be substantially reduced through system-level hybridization, shifting the design focus from component sizing to configuration selection. Five configurations are evaluated for a calibrated rural mini-grid (175 kWh/day, 50 kW peak) using HOMER Pro under consistent reliability constraints. Two dimensionless indices are introduced for cross-configuration assessment: the Battery Capacity Reduction Index (BCRI) and Emission Reduction Index (ERI).

Progressive hybridization reduces required battery capacity from 250 kWh in the photovoltaic-only baseline to 50 kWh in the full hybrid configuration (BCRI = 0.80). The levelized cost of energy decreases from \$0.236 to \$0.102 per kWh (INR 21.25 to INR 9.18), corresponding to a 56.8% reduction. The cost-optimal configuration achieves a 100% renewable fraction and zero direct CO_2 emissions (ERI = 1.00). Sensitivity analyses confirm that the cost ranking remains robust under variations in discount rate, fuel price, irradiance, and biomass feedstock cost.

The study contributes: (i) a stepwise hybridization framework for isolating the structural effect of hybridization on storage demand; (ii) transferable comparative indices for cross-study assessment; and (iii) a cleaner-production perspective linking configuration choice to reductions in upstream battery-material demand and end-of-life burden. The framework supports comparative sustainable energy technology assessment for rural electrification planning.

Keywords: Hybrid renewable energy systems, Renewable mini-grids, Battery energy storage, Material efficiency, Rural electrification, Techno-economic assessment, HOMER Pro, Hybridization.

May 26, 2026

1. Introduction

1.1. Energy access challenge and the role of decentralized renewables

Universal and reliable access to electricity remains an unresolved development challenge for several hundred million people worldwide, predominantly in rural and peri-urban communities of South Asia and Sub-Saharan Africa [1, 2]. The geographic and economic constraints that limit grid extension to these communities are well documented. These include low population density, dispersed settlement patterns, difficult terrain, and the high specific cost of last-mile distribution infrastructure [3, 4, 5]. In such settings, decentralized renewable energy (DRE) systems based on solar photovoltaic (PV), wind, biomass, and small hydropower show an economically and technically credible alternatives to centralized grid expansion [6, 7]. Solar energy systems are increasingly being explored for decentralized agricultural and rural energy applications in India due to their scalability, declining cost, and suitability for distributed deployment [8].

In India, the country setting of the present study, the policy environment for DRE has steadily strengthened. The national target of 500 GW of non-fossil installed capacity by 2030, combined with the Ministry of New and Renewable Energy's draft mini-grid policy and several state-level rural electrification programs, has placed DRE mini-grids at the center of the country's energy transition [9, 10]. Recent techno-economic assessments confirm that hybrid mini-grids are increasingly cost-competitive with grid extension at the village scale [11, 12, 13].

1.2. Battery storage as the principal cost and material bottleneck

Despite favorable resource availability and declining solar PV costs, the economics of off-grid renewable mini-grids continue to be dominated by the capital and replacement cost of energy storage. Lithium-ion battery banks now constitute between 50% and 60% of the capital expenditure of typical PV-only rural systems, depending on the autonomy requirement and the battery chemistry [14, 11, 15]. Although the price of lithium-ion battery packs has fallen substantially over the past decade, the rate of decline has been slower than that of crystalline silicon PV modules. The consequence is that storage now represents a larger relative share of mini-grid capital cost than it did a decade ago [14, 16].

The economic burden of storage is accompanied by a substantial upstream material burden. Lithium-ion battery manufacturing depends on geographically concentrated supply chains for lithium, cobalt, nickel, and graphite, with associated extractive impacts and geopolitical risks [17, 18]. Recent lifecycle assessment studies of PV-battery systems further highlight the environmental implications associated with large-scale battery deployment [19]. Li et al. [20] compared multiple large-scale energy storage technologies on techno-economic grounds, demonstrating that storage selection has major cost implications for renewable energy integration. The complementary question, how storage requirements themselves respond to system architecture, has received comparatively less attention in the literature. End-of-life management of large stationary

battery systems also remains unresolved in many rural deployment contexts, where formal collection, recycling, and recovery infrastructure is limited. Reducing installed battery capacity at the design stage therefore offers three coupled benefits: lower capital cost, reduced upstream material demand, and lower end-of-life waste burden. This aligns with the broader sustainability and economic objectives associated with renewable energy transition pathways [21].

This framing motivates a research question that has not been adequately addressed in the existing literature: *to what extent can the storage requirement of a rural renewable mini-grid be reduced by changing the architecture of the system, before component sizing or cost optimization?* The present study investigates this question through a comparative simulation of five hybrid renewable configurations.

1.3. Hybridization hypothesis and resource complementarity

The theoretical basis for storage reduction through hybridization rests on the concept of resource complementarity. When two or more renewable resources have temporally complementary generation profiles, their combined output more closely matches a typical load than either source alone, reducing the storage required to buffer the mismatch [22, 23, 24]. The mechanism is intuitively simple. When a second source produces energy during periods when the first is weakest, the deficit no longer needs to be bridged from storage. Each additional complementary source thus substitutes generated energy for stored energy.

Empirical studies have documented this complementarity at multiple spatial and temporal scales. PV and wind generation are complementary at diurnal and seasonal time scales in many tropical and subtropical sites [25, 23, 26]. PV and biomass are complementary in the dispatchability dimension: biomass can be called on demand to fill PV deficits, including extended monsoon or overcast sequences [27, 28, 29]. PV and small hydropower are complementary at seasonal scale where the rainfall pattern is anticorrelated with the dry-season solar peak [22, 30]. Recent reviews further emphasize that hybrid renewable energy systems improve reliability, storage utilization, and grid stability through coordinated integration of complementary renewable resources and energy storage technologies [31]. The combined system can therefore reduce storage and increase reliability simultaneously, departing from the traditional assumption that the two are traded off against each other.

1.4. Cleaner production framing

The hybridization-as-storage-substitution mechanism connects naturally to the cleaner production paradigm. The cleaner production framework, as articulated in early formulations and elaborated through the circular economy literature, treats waste prevention at the design stage as the most effective intervention in the materials hierarchy [32, 33, 34]. End-of-pipe mitigation accepts waste as inevitable and treats it after the fact. Design-stage prevention, by contrast, eliminates waste before it arises by changing the structure of the producing system.

Architecture-based hybrid system design fits this latter category. The choice of system configuration determines the lifetime material intensity of the deployed mini-grid before any component is procured or installed. A configuration that requires 80% less battery capacity than its single-source baseline reduces upstream demand for storage materials by approximately the same proportion. None of this reduction requires subsequent recycling, recovery, or end-of-life treatment. The benefit is captured by not building the storage in the first place. The cleaner production framework provides the appropriate language for interpreting hybridization as a structural intervention in material flows, not merely as an engineering optimization for cost or reliability.

1.5. Research gap, objectives, and contribution

Three gaps in the existing literature motivate the present study. First, although individual hybrid configurations have been extensively analyzed, comparative studies that evaluate multiple architectures under *consistent* assumptions to isolate the hybridization effect are scarce [15, 12]. Most HOMER-based studies report a single optimum and its sensitivity, but do not explicitly compare architectures along a graduated hybridization ladder. Second, the cleaner production framing of hybrid mini-grid design is rarely articulated in the techno-economic literature; most studies treat cost reduction and emission reduction separately, and neither is typically connected to upstream material flows. Third, dimensionless metrics for comparing storage reduction and emission reduction across studies are not standard, which limits cross-study synthesis.

The literature comparison underpinning these gaps is drawn from techno-economic studies of hybrid renewable mini-grids published between 2008 and 2026 and indexed in Scopus and Web of Science. Studies were selected on the basis of (i) explicit treatment of off-grid or weak-grid mini-grids at the village or institutional scale, (ii) inclusion of solar photovoltaic with at least one additional generation source, and (iii) reporting of levelized cost of energy or net present cost. The 49 references retained for this comparative study span foundational complementarity theory, simulation methodology, regional resource assessment, and recent multi-source case studies relevant to the South Asian and African contexts.

The objectives of the present study are therefore:

- O1. To simulate five feasible HRES configurations for a calibrated rural Indian site under consistent techno-economic and reliability assumptions, and to identify the cost-optimal architecture.
- O2. To introduce two dimensionless indices, the Battery Capacity Reduction Index (BCRI) and the Emission Reduction Index (ERI), that permit configuration-independent comparison of storage and emission performance.
- O3. To interpret the comparative outcomes within the cleaner production framework and to identify implications for the material intensity of rural electrification.

The contributions of the study are correspondingly threefold. First, progressive hybridization is quantified as a coupled reduction of storage and cost, rather than as a

trade-off between cost and reliability. Second, the BCRI and ERI indices are formally defined and applied to support cross-study comparison. Third, the cleaner production interpretation positions hybridization as a design-stage pollution prevention intervention with direct implications for upstream material flows in rural mini-grid deployment.

The remainder of this paper is organized as follows. Section 2 describes the case site, the five configurations evaluated, the simulation framework, the cost and performance parameters, and the dimensionless indices. Section 3 presents the optimization outcomes and the sensitivity analyses. Section 4 interprets the results within the cleaner production framework and the published literature. Section 5 summarizes the principal findings and identifies directions for future work.

2. Methodology

This section describes the techno-economic optimization framework used to evaluate the five HRES configurations. The site, load, and resource characterization are presented first (Section 2.1), followed by the configuration set (Section 2.2), the simulation framework (Section 2.3), the component cost and performance parameters (Section 2.4), the dimensionless indices (Section 2.5), and an explicit treatment of the modeling framework's limitations (Section 2.6).

2.1. Site, load, and resource characterization

The case study site is a rural educational and skill-development institute in Maharashtra, India (Vigyan Ashram, Pabal: 18.837°N, 74.058°E, 630 m above mean sea level). The institute serves a combined load comprising classrooms, residential hostels, vocational workshops, and agricultural pumping during the cropping season. The load is therefore representative of productive-use rural mini-grids, and is more diverse and variable than residential-only systems typical of household-scale electrification.

The annual design load was triangulated from four independent sources to ensure calibration robustness. The first source was twelve months of MSEDCL (Maharashtra State Electricity Distribution Co. Ltd.) utility billing data, which provided the existing aggregate consumption and load factor. The second source was a bottom-up appliance-level summation, in which each electrical device on the campus was inventoried with its rated power and daily operating hours. The third source was a peak-demand utilization analysis based on observed simultaneity factors. The fourth source was a forward-looking scaling factor of 3.0 applied to the current billing-derived consumption, capturing the planned expansion of productive-use activity. The four estimates converged on a design daily load of 175 kWh/day with a peak demand of 50 kW. The annual energy demand is therefore 63,875 kWh/yr, and the design load factor is 0.146.

Solar resource data were retrieved from the NASA POWER database for the site coordinates. The annual average global horizontal irradiance (GHI) is 5.13 kWh/m^2/day,

with a peak in March (6.78 kWh/m^2/day) and a trough in July (3.42 kWh/m^2/day) coinciding with the southwest monsoon. Wind resource data, also from NASA POWER, give an annual average wind speed of 4.50 m/s at 10 m above ground level. Wind speed extrapolation to the 20 m hub height assumed for the candidate turbine was carried out using the Hellmann power law with an exponent of 0.143, appropriate for open terrain [35, 36]. Local biomass availability was assessed from monthly agricultural residue surveys in the surrounding Shirur Taluka, including bagasse, rice straw, sorghum stalks, and sugarcane tops. The aggregate annual availability is approximately 420 tonnes/yr, with a clear seasonal profile peaked in November and minimum in March [29, 28].

2.2. HRES configurations evaluated

Five configurations are evaluated under common load and resource inputs. The configurations are designed to span a progressive hybridization ladder from single-source PV to a four-component full hybrid (Table 1). Case 1 is the PV-plus-battery baseline. Case 2 introduces a diesel generator as a fossil-fueled firm-capacity backup, providing a benchmark against the most common fossil-hybrid design in the literature [37, 38, 39]. Case 3 substitutes the diesel with a small wind turbine, and Case 4 substitutes it with a biomass gasifier. Case 5 combines all three renewable sources with a battery in the full hybrid system. Figure 1 shows the schematic for this.

Table 1: The five HRES configurations evaluated, spanning the progressive hybridization ladder from single-source PV to four-component full hybrid.

Case	**Architecture**	**Role**
Case 1	PV + Battery	Single-source baseline
Case 2	PV + Diesel + Battery	Fossil-hybrid benchmark
Case 3	PV + Wind + Battery	Renewable dual-source A
Case 4	PV + Biomass + Battery	Renewable dual-source B
Case 5	PV + Wind + Biomass + Battery	Full renewable hybrid

The exclusion of small hydropower from the evaluated set reflects the absence of perennial streamflow at the case site. Hydrogen-electrolyzer storage is also excluded because its capital cost is not yet competitive at the load scale of this study [40, 41]. The five-case set therefore captures the full set of feasible renewable architectures at the case site under current technology costs.

2.3. HOMER Pro simulation framework

This study does not aim to introduce a new optimization algorithm; rather, it isolates the structural effect of hybridization on storage and cost under controlled, consistent assumptions. The HOMER Pro tool is used as the analytical engine because of its established role in mini-grid techno-economic studies and the reproducibility of its hourly energy-balance and lifecycle cost framework.

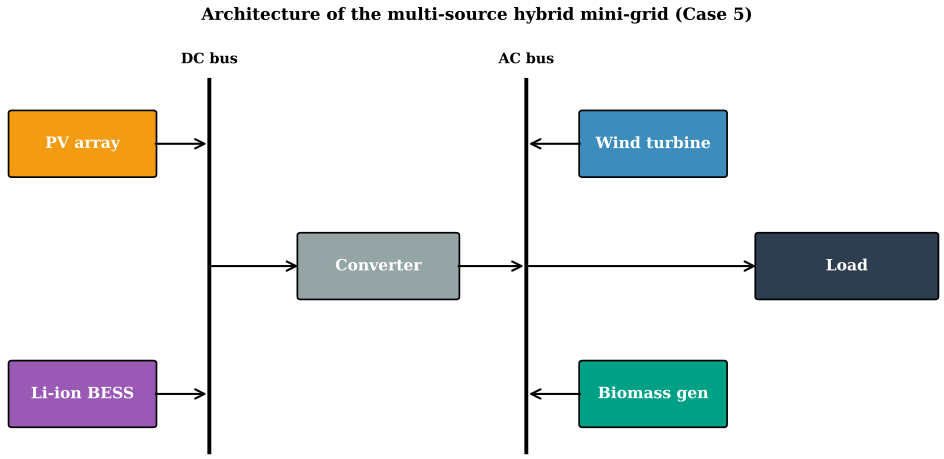


Figure 1: Schematic of the Case 5 full-hybrid architecture: PV array, small wind turbine, biomass gasifier, lithium-ion battery bank, and bidirectional converter serving the AC load. The diagram is conceptual; component sizes (50 kW PV, 20 kW wind, 5 kW biomass, 50 kWh battery, 50 kW converter) are the HOMER-optimized values. Component sizes are reported in Table 1. Cases 1 to 4 are obtained as architectural subsets by removing specific components.

All five configurations are simulated using HOMER Pro (version 3.18.4) [42, 43], a widely used hybrid energy systems simulation tool that performs hourly energy balance across an 8,760-hour annual cycle and lifecycle cost optimization across a project lifetime of 25 years. HOMER has been extensively applied in the rural electrification literature for techno-economic assessment of hybrid configurations [11, 13, 15, 26, 44].

The optimization minimizes net present cost (NPC) over the project lifetime subject to a reliability constraint. The reliability constraint adopted in this study is a maximum loss of power supply probability (LPSP) of 1%, equivalent to a maximum annual capacity shortage of 1% of total annual load. The 1% threshold is consistent with productive-use rural mini-grid standards reported in the international literature and is stricter than the typical residential-scale threshold of 5% [5, 12]. Levelized cost of energy is computed as

$$\mathrm{LCOE} = \frac{\mathrm{NPC} \cdot \mathrm{CRF}(i, N)}{E_{\mathrm{served}}} \tag{1}$$

where $\mathrm{CRF}(i, N)$ is the capital recovery factor at real discount rate i over project lifetime N, and E_{served} is the total annual energy served. Renewable fraction is computed as

$$\mathrm{RF} = 1 - \frac{E_{\mathrm{nonren}}}{E_{\mathrm{served}}} \tag{2}$$

where E_{nonren} is annual non-renewable generation (diesel-only, in this study).

For each configuration, two dispatch strategies were evaluated and the lower-LCOE outcome retained: load-following (LF), in which dispatchable generators serve only current load, and cycle-charging (CC), in which dispatchable generators run at rated output and charge the battery from any surplus. LF was selected for Cases 1 and 4 (renewable-only with biomass dispatchable on demand). CC was selected for Cases 2, 3, and 5 (in which a stochastic or fossil-fueled source operates more efficiently at rated load and benefits from battery charging).

The optimization search space was iteratively expanded for each configuration until the cost-optimal solution lay strictly in the interior of the search space and HOMER's border warnings were absent [42]. This protocol ensures that the reported optima are not artifacts of search-space boundary imposition.

2.4. Component cost and performance parameters

Component costs were derived from a combination of vendor quotations collected during April 2026 in the Pune–Mumbai industrial corridor and authoritative international benchmarks where local data were not available [14, 9, 43]. The techno-economic parameters used in all five configurations are summarized in Table 2. All capital costs are reported in United States dollars; the exchange rate of INR 90 per USD (Early 2026) is applied for INR-denominated outputs.

Table 2: Component techno-economic parameters used in the optimization. All costs are nominal April 2026 values in United States Dollars ($), derived from vendor quotations and Indian-market benchmarks. All five configurations use identical parameters and differ only in component selection and sizing [1, 14].

Component	**Capital** ($/unit)	**Replacement** ($/unit)	**O&M** ($/unit/yr)	**Lifetime** (yr or h)
PV array (per kW)	$500	$400	$10/yr	25 yr
Lithium-ion battery (per kWh)	$350	$280	$5/yr	15 yr
Bidirectional converter (per kW)	$200	—	—	15 yr
Diesel generator (per kW)	$300	—	$0.03/h	15,000 h
Wind turbine (per kW)	$1,100	$950	$30/yr	20 yr
Biomass gasifier (per kW)	$1,200	$1,000	$0.04/h	15,000 h

The PV system is modeled as a fixed-tilt monocrystalline silicon array at 18° tilt facing south, with an overall derating factor of 80% applied to capture soiling (5%), wiring and mismatch losses (5%), temperature derating (7%), and degradation over the 25-year lifetime (3%) [45]. The bidirectional converter is fixed at 50 kW across all configurations to match the peak load and reduce optimization dimensionality.

The battery bank is lithium iron phosphate (LFP) chemistry, selected for three reasons relevant to rural mini-grid applications [46]. First, the round-trip efficiency of 95%

reduces the PV oversizing required to charge a given storage capacity. Second, the allowable depth of discharge of 80% (minimum SOC of 20%) effectively doubles the usable capacity per kWh of installed capacity relative to typical lead-acid systems. Third, the rated cycle life of 4,000–6,000 cycles at 80% depth of discharge eliminates the need for mid-life battery replacement under the expected annual cycling regime, improving 25-year lifecycle economics.

The biomass gasifier in Cases 4 and 5 operates on dry agricultural residue with a lower heating value of 15.5 MJ/kg and a local delivered cost of INR 2/kg ($0.022/kg). The electrical efficiency at rated load is approximately 22%, yielding a fuel consumption rate of approximately 1.30 kg/kWh of electrical output. The minimum load ratio is set at 50%; below this threshold the dispatch logic holds the gasifier offline [29, 28].

For fossil-fueled generators (Case 2), HOMER applies a combustion emission factor of 2.64 kg CO_2 per liter of diesel. For biogenic biomass fuels (Cases 4 and 5), the operational CO_2 emission factor is set to zero, following the biogenic carbon-neutrality convention of the IPCC [47]. The biogenic neutrality convention is a simplification relative to full life-cycle analysis but is the standard treatment in the biomass and bioenergy techno-economic literature [28, 29].

2.5. Dimensionless indices for cross-configuration comparison

To enable comparison across configurations and across studies that may differ in absolute scale, two dimensionless indices are introduced. The Battery Capacity Reduction Index (BCRI) is defined relative to a PV-only baseline, and the Emission Reduction Index (ERI) is defined relative to a diesel-hybrid reference:

$$\mathrm{BCRI}_i = 1 - \frac{C_i}{C_{\mathrm{PV}}}, \qquad \mathrm{ERI}_i = 1 - \frac{E_i}{E_{\mathrm{DG}}}. \tag{3}$$

In equation (3), C_i is the optimized battery capacity of configuration i, C_{PV} is the optimized battery capacity of the PV-only baseline (Case 1) under identical load and reliability constraints, E_i is the annual operational CO_2 emissions of configuration i, and E_{DG} is the corresponding emissions of the diesel hybrid reference (Case 2). Both indices are bounded between 0 (no improvement over the respective baseline) and 1 (complete elimination of storage requirement or operational emissions). They are dimensionless and architecture-invariant, enabling comparison across configurations and across studies with different absolute load and cost scales.

2.6. Limitations of the modeling framework

The HOMER Pro framework provides design-stage screening of hybrid configurations through hourly energy balance and lifecycle cost optimization. The framework does not model sub-hourly dispatch dynamics, partial-load efficiency, control and protection coordination, battery aging under cycling regimes, or social and institutional factors that influence deployment. Component costs reflect Early 2026 vendor quotations and

Indian-market benchmarks; sustained price shifts in lithium-ion modules in particular would alter the absolute LCOE but not the relative ordering of configurations. A consolidated treatment of all modeling limitations, resource and cost-input uncertainties, and deployment-stage factors not captured by the framework is provided in Section 4.5.

3. Results

This section presents the optimization outcomes of the five configurations under the unified evaluation framework defined in Section 2. The structure follows the logical chain of the hybridization argument: first the headline storage and cost reduction (Sections 3.1–3.3), then the environmental performance and the dimensionless indices that quantify these reductions in a configuration-independent way (Sections 3.4–3.5), then the operational behavior of the cost-optimal architecture (Section 3.6), and finally the sensitivity tests that establish the robustness of the comparative findings (Section 3.7).

3.1. Optimization outcomes across the five configurations

Table 3 consolidates the optimal architecture and techno-economic outcome of each configuration. All five cases satisfy the LPSP $\leq 1\%$ reliability constraint. The optimization identified an interior optimum within the search space for every case, after iterative expansion of the boundary dimensions until no border warning remained.

Three patterns are immediately evident from the master table. First, the PV array size in the cost-optimal configurations is *not* monotonic with the number of resources: it falls from 120 kW in Case 1 (PV-only baseline) to 50 kW in Case 5 (full hybrid). Adding generation diversity allows the optimizer to downsize the single most expensive generation component. Second, the battery bank contracts monotonically from 250 kWh to 50 kWh as additional generation sources are integrated. Third, the levelized cost of energy declines monotonically from \$0.236/kWh in Case 1 to \$0.102/kWh in Case 5, a 56.8% reduction.

3.2. Progressive battery storage reduction

The battery storage requirement falls from 250 kWh in the single-source baseline to 50 kWh in the full hybrid, a reduction of 80% (Fig. 2). The reduction is not linear in the number of resources. Adding any one of three options to the PV-only baseline (a diesel generator in Case 2, a wind turbine in Case 3, or a biomass gasifier in Case 4) reduces storage to 100 kWh in all three cases, a uniform 60% reduction. This convergence to the same battery size, despite differing resource types, indicates that the storage requirement of Case 1 is dominated by a specific kind of deficit (multi-day monsoon cloud sequences) rather than total annual energy shortfall. Any source capable of bridging this multi-day deficit reduces the battery size to the same value.

The further reduction from 100 kWh to 50 kWh in Case 5 is achieved not by adding a fourth resource of the same kind but by combining two resources whose dispatch

Table 3: Master techno-economic comparison of the five HRES configurations. All cases satisfy LPSP $\leq 1\%$ over a 25-year project lifecycle. Costs are reported in United States dollars ($); the INR equivalent is provided for the LCOE row to enable comparison against the local grid tariff. The cost-optimal configuration is highlighted.

Metric	**Case 1** PV+B	**Case 2** PV+DG+B	**Case 3** PV+W+B	**Case 4** PV+Bio+B	**Case 5** ⋆ Full hybrid
Architecture					
PV (kW)	120	80	120	80	50
Wind (kW)	—	—	10	—	20
Diesel (kW)	—	22	—	—	—
Biomass gasifier (kW)	—	—	—	10	5
Battery (kWh)	250	100	100	100	**50**
Converter (kW)	50	50	50	50	50
Costs					
CAPEX ($ thousand)	158	92	116	97	**61**
NPC ($ thousand)	228	152	160	152	**99**
LCOE ($/kWh)	0.236	0.157	0.165	0.157	**0.102**
LCOE (INR/kWh)	21.25	14.13	14.88	14.16	**9.18**
Environmental and reliability					
Renewable fraction (%)	100	92.2	100	100*	100
CO_2 (kg/yr)	0	3,882	0	0*	0
Battery autonomy (h)	27.4	11.0	11.0	11.0	5.5

* Case 4 RF and CO_2 reflect IPCC biogenic-neutrality treatment of biomass combustion.

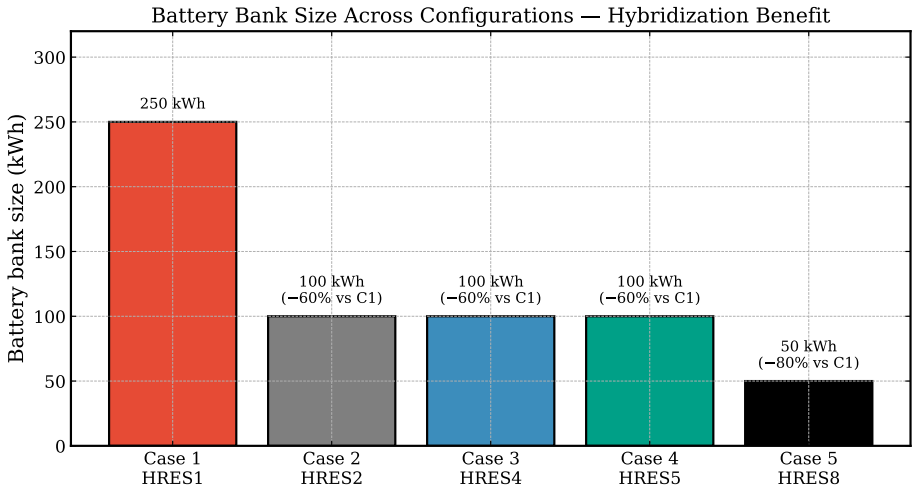


Figure 2: Optimal battery bank capacity across the five configurations, from HOMER Pro optimization output. Each addition of a complementary or dispatchable source to the PV baseline reduces storage from 250 kWh to 100 kWh (a uniform 60% reduction across Cases 2, 3, 4). The full multi-source hybrid (Case 5) reaches 50 kWh, an 80% reduction relative to the PV-only baseline.

profiles are complementary. Wind covers the daytime and evening hours of the monsoon season, while biomass provides firm capacity for sustained cloud sequences when wind is also weak. Each resource thus relieves a different part of the storage burden, and the optimizer can size the battery for diurnal cycling alone. Figure 3 shows the joint trajectory of battery size and LCOE across the five configurations, making the substitution of generated energy for stored energy visible as a single curve.

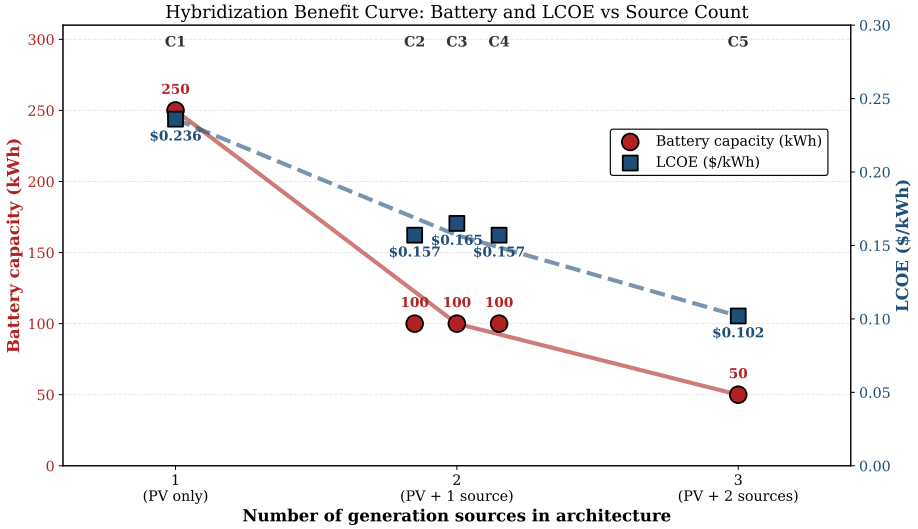


Figure 3: Hybridization benefit curve. Each configuration is plotted at the number of generation sources in its architecture: Case 1 has one source (PV only), Cases 2–4 have two sources (PV plus one addition), and Case 5 has three. The left axis (red, solid) shows the HOMER-optimized battery capacity; the right axis (blue, dashed) shows the corresponding levelized cost of energy. Both metrics decline simultaneously. This indicates that hybridization substitutes storage and reduces cost together rather than trading one for the other. Connecting lines are visual aids between simulated points, not interpolated values.

3.3. Economic performance and capital decomposition

The economic outcomes of the five cases occupy three distinct clusters (Fig. 4). Case 1 is the high-cost outlier at \$0.236/kWh. Cases 2, 3, and 4 cluster within \$0.157–0.165/kWh, separated by less than \$0.008/kWh. Case 5 separates downward to \$0.102/kWh, the only configuration that is comparable to current MSEDCL grid tariff band of INR 10–12/kWh (\$0.111–0.133/kWh). The NPC profile mirrors the LCOE structure because the load and lifecycle are identical across cases.

The capital decomposition (Fig. 5) reveals where hybridization saves money. The battery share of CAPEX falls from 56% in Case 1 to 29% in Case 5. PV remains the largest single component throughout, but its absolute size shrinks. Auxiliary generation (diesel, wind, or biomass) accounts for between 4% and 12% of CAPEX in Cases 2–5, a small marginal investment relative to the storage savings it enables. The total CAPEX falls from \$158,000 in Case 1 to \$61,000 in Case 5, a reduction of 61.5%.

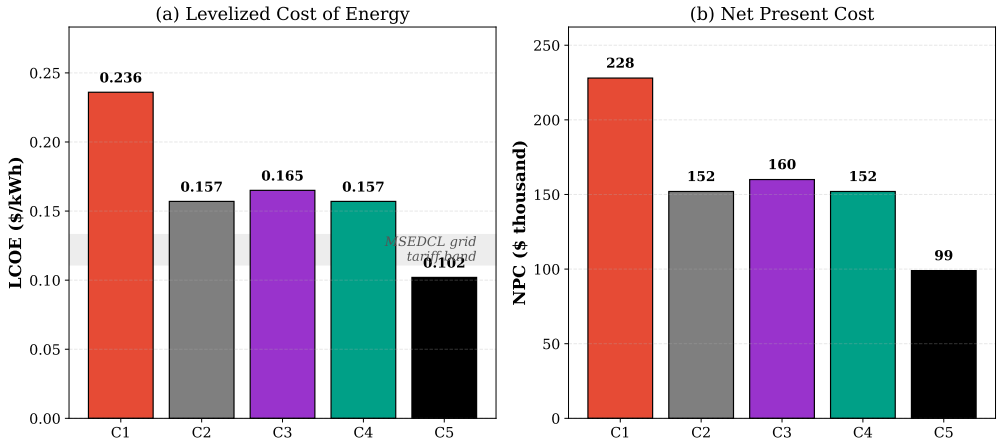


Figure 4: Levelized cost of energy (panel a, left) and net present cost (panel b, right) for the five configurations, from HOMER Pro optimization results. The grey horizontal band in panel a marks the contemporary MSEDCL commercial tariff range (\$0.111–\$0.133/kWh). Only Case 5 (\$0.102/kWh) comes around this band. All configurations satisfy LPSP $\leq 1\%$ over the 25-year project lifecycle.

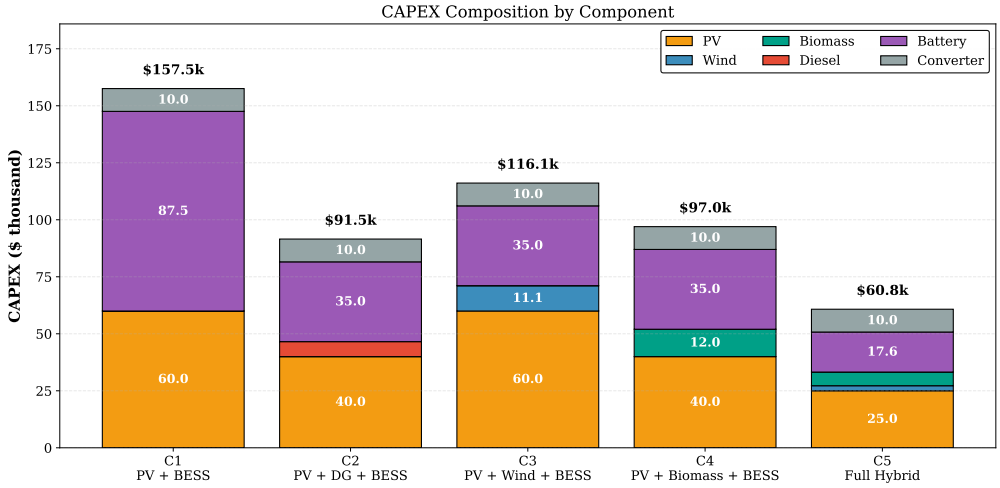


Figure 5: Capital expenditure decomposition by component for the five configurations, in United States dollars (thousand). The battery share declines from 56% in Case 1 to 29% in Case 5; auxiliary generation captures 4–12% of CAPEX across cases. Total CAPEX is reduced by 61.4% from Case 1 (\$157.5k) to Case 5 (\$60.8k). Numbers on each segment are component CAPEX in \$ thousand; numbers above each bar are case totals.

3.4. Environmental performance

Four of the five configurations achieve a renewable fraction of 100% and zero direct CO_2 emissions (Fig. 6). Case 2 is the sole exception: it produces 3,882 kg CO_2/yr from 1,471 L of diesel consumed during 240 hours of generator operation. The diesel runtime is concentrated in July through September, the period of weakest solar resource, and accounts for only 2.7% of the 8,760-hour year. Even this limited operation is sufficient to differentiate Case 2 sharply from Cases 3, 4, and 5 on environmental performance: a single fossil-fueled generator, however briefly run, places the configuration in a different category from the renewable-only hybrids.

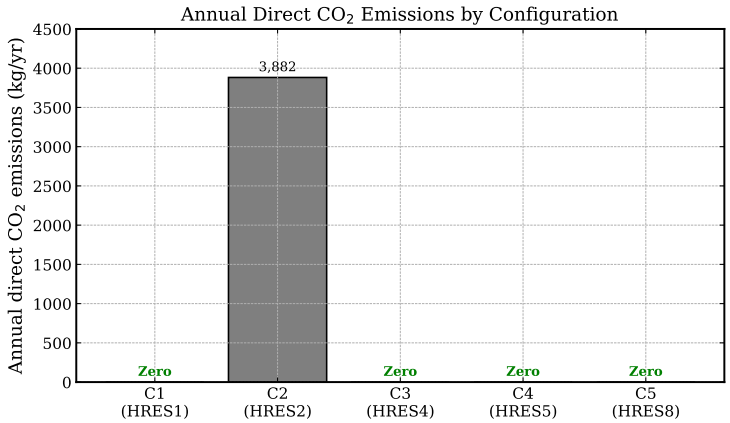


Figure 6: Annual direct CO_2 emissions for the five configurations, from HOMER fuel-consumption output. Cases 1, 3, 4, and 5 emit zero CO_2 directly because no fossil fuel is consumed. Case 2 emits 3,882 kg/yr from 1,471 L of diesel consumed during monsoon backup. Biomass combustion in Cases 4 and 5 is treated as biogenic-neutral per IPCC convention; upstream and combustion-side caveats are discussed in Section 4.

3.5. Dimensionless indices: BCRI and ERI

Section 2.5 introduced two dimensionless indices to permit configuration-invariant comparison. Their values for the five cases are:

$$\mathrm{BCRI}_i = 1 - \frac{C_i}{C_{\mathrm{PV}}}, \qquad \mathrm{ERI}_i = 1 - \frac{E_i}{E_{\mathrm{DG}}}, \tag{4}$$

where C_i and E_i are the optimized battery capacity and annual CO_2 emissions of configuration i, with the PV-only baseline ($C_{\mathrm{PV}} = 250$ kWh) and the diesel-hybrid ($E_{\mathrm{DG}} = 3{,}882$ kg/yr) as the reference denominators. The indices are bounded between 0 (no improvement over the respective baseline) and 1 (complete elimination of storage or emissions). Table 4 summarizes the values.

The simultaneous achievement of both indices is the central quantitative result of the study. Case 5 is the only configuration with BCRI ≥ 0.80 *and* ERI $= 1.00$. Cases 3 and 4 reach ERI $= 1.00$ but stop at BCRI $= 0.60$. Case 2 reaches BCRI $= 0.60$ but fails

Table 4: Dimensionless storage and emission reduction indices. BCRI is computed against the PV-only baseline; ERI against the diesel-hybrid emissions reference.

Index	Case 1	Case 2	Case 3	Case 4	Case 5
BCRI	0.00	0.60	0.60	0.60	**0.80**
ERI	1.00	0.00	1.00	1.00	**1.00**

on emissions (ERI = 0.00). The radar visualization in Fig. 7 extends this comparison to five normalized axes (LCOE, NPC, RF, BCRI, CO_2 score). Case 5 forms the outer envelope on every axis. No other case achieves non-dominance.

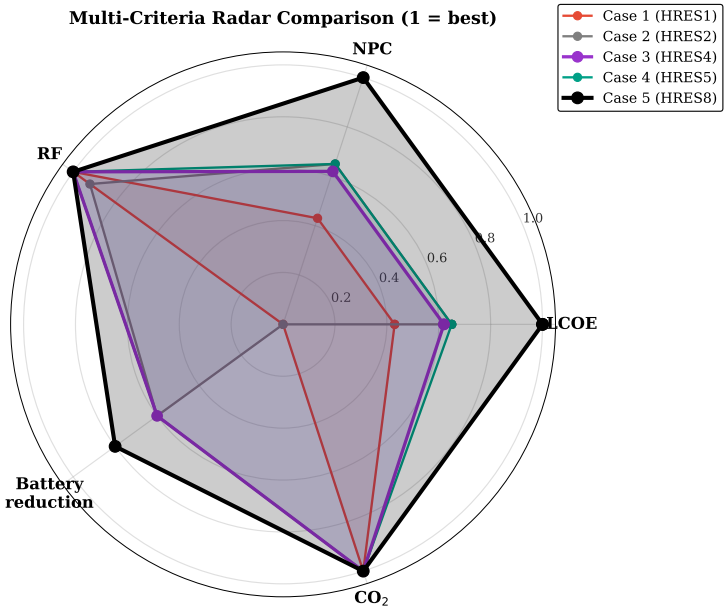


Figure 7: Five-axis multi-criteria comparison across configurations. The axes are: LCOE, NPC, renewable fraction (RF), battery reduction (BCRI), and CO_2 reduction (ERI). Each axis is normalized so that 1.0 represents the best performance across the five cases. Case 5 forms the outer envelope on every axis and is non-dominated under the chosen criteria. Case 2 collapses on the CO_2 axis because diesel combustion produces direct emissions absent from the renewable-only configurations.

3.6. Operational behavior of the full hybrid (Case 5)

The aggregated annual figures above conceal the operational dynamics that allow Case 5 to achieve its low storage and cost. Figure 8 shows an hour-resolved dispatch profile for a representative monsoon week. PV serves the daytime load, wind reinforces the morning and evening shoulder hours, biomass is dispatched during nighttime and overnight gaps, and the battery absorbs short-term fluctuations rather than multi-day deficits. The dispatch sequence demonstrates the temporal complementarity that the annual energy mix obscures.

The biomass consumption associated with Case 5 is 12.15 tonnes/yr, or 2.9% of the

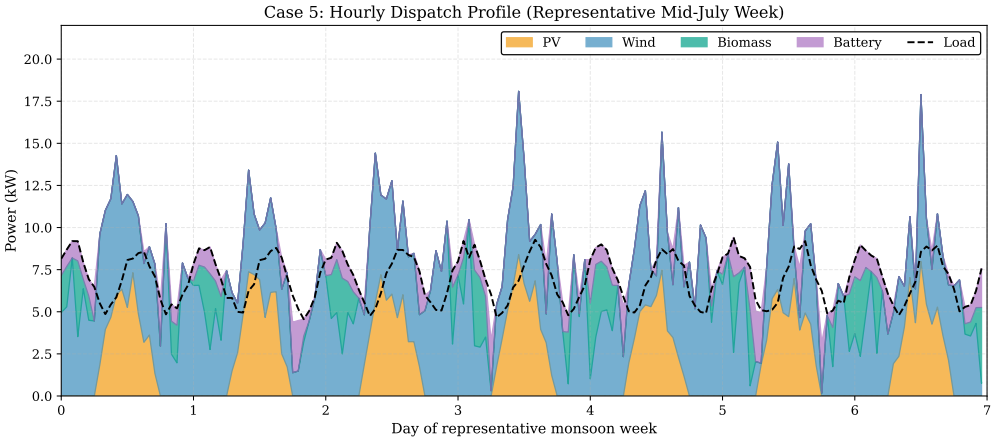


Figure 8: Hour-resolved representative dispatch profile for Case 5 during a monsoon week. An illustrative figure constructed to show the qualitative dispatch logic. PV (orange) covers the daytime peak, wind (blue) reinforces shoulder hours, biomass (teal) provides dispatchable backup during night and overnight deficits, and the battery (purple) absorbs the residual cycling mismatch. The load curve (dashed) is the profile used in the simulation. Specific peaks and troughs vary with weather realizations and dispatch-strategy parameters.

locally assessed availability of 420 tonnes/yr at the case site. Fig. 9 shows the monthly availability profile against the consumption profile. The largest monthly consumption (2.0 tonnes in August, dispatched during sustained monsoon cloud cover) remains comfortably below even the lowest monthly availability (6 tonnes in July). The two orders of magnitude margin between availability and consumption is a critical indicator of feedstock security at this site, although the margin itself is not transferable to sites with weaker agricultural-residue production.

3.7. Sensitivity and robustness of the comparative findings

The comparative findings depend on the input parameters used in the optimization. To assess robustness, four parameters were varied independently: real discount rate (8–14%), diesel fuel price (±30%), solar GHI (±20%), and biomass feedstock cost (±25%). The results are summarized in Table 5 and visualized in the tornado diagram (Fig. 10).

The cost ranking of the five cases is stable across the entire tested parameter space. Case 5 remains the cost-optimal configuration in every sensitivity scenario. Case 1 remains the most expensive in every scenario. The ordering of Cases 2, 3, and 4 is stable for discount rates between 9% and 13%, and reorders only at the extremes of the range. Diesel fuel price affects only Case 2: a 30% diesel price increase raises Case 2 LCOE by approximately \$0.018/kWh (Fig. 11), erasing its current \$0.008/kWh advantage over Case 3 and bringing it to within \$0.002/kWh of Case 4. The renewable-only configurations are immune to fuel-price variation by design.

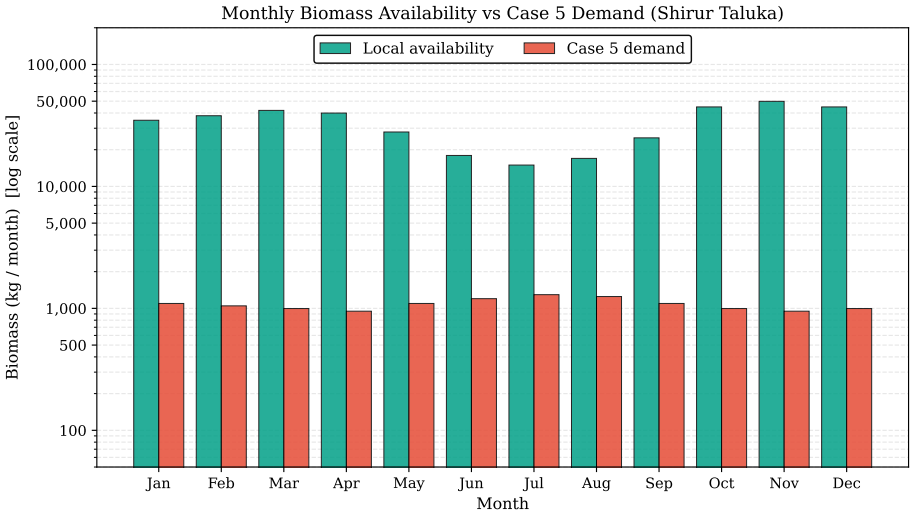


Figure 9: Monthly biomass availability (logarithmic scale) (green bars, left scale) compared to the HOMER-derived monthly demand (consumption) for the gasifier in Case 5. The indicative availability profile is constructed from typical agricultural-residue seasonality in the region. Availability exceeds demand by approximately one to two orders of magnitude across all months, indicating that feedstock supply is not a binding constraint.

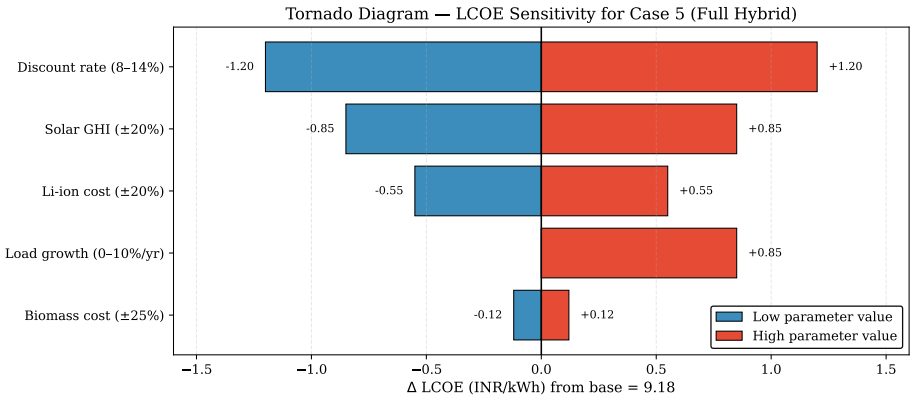


Figure 10: Tornado diagram of LCOE sensitivity for the cost-optimal configuration (Case 5). Bar length represents the LCOE swing from low to high parameter values. Discount rate exerts the largest influence; diesel price exerts none because Case 5 contains no diesel.

Table 5: Sensitivity summary for the cost-optimal configuration (Case 5). LCOE swing for each input parameter varied independently within the indicated range.

Parameter	**Range tested**	**LCOE swing**	**Cost-rank stable?**
Real discount rate	8%–14%	±$0.016/kWh	Yes
Diesel fuel price	±30%	0 (no diesel)	Yes
Solar GHI	±20%	±$0.012/kWh	Yes
Biomass cost	±25%	±$0.003/kWh	Yes

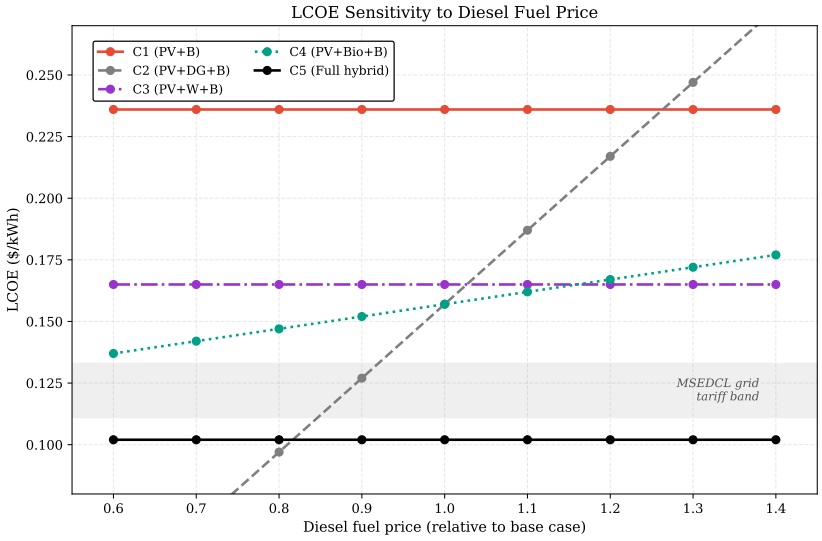


Figure 11: Sensitivity of LCOE to diesel fuel price across the five configurations. Cases 1, 3, and 5 are flat (no fuel-price dependence by design). Case 2 rises linearly with diesel price, exposing the diesel-hybrid configuration to fuel-price risk that the renewable-only configurations avoid. The horizontal band indicates the contemporary MSEDCL grid tariff range.

4. Discussion

The Results section establishes that progressive hybridization reduces both battery storage and levelized cost simultaneously while maintaining a 100% renewable fraction in the multi-source case. This section interprets these findings in four dimensions: the underlying mechanism (Section 4.1), the literature context (Section 4.2), the cleaner production framing (Section 4.3), and the cost-emission trade-off space (Section 4.4). Sections 4.5 and 4.6 treat the limitations of the study and the practical implications for planners, respectively.

4.1. The hybridization mechanism: substitution of generated for stored energy

The simultaneous reduction of storage and cost across the configuration sequence is not coincidental. The two are coupled through the energy-balance constraint of the system. The PV-only baseline (Case 1) must store, in the form of battery capacity, every kilowatt-hour of energy demand that is not coincident with solar generation. The largest such demand windows are the multi-day monsoon cloud sequences, during which battery capacity must be sized for several days of autonomous operation. The 250 kWh battery of Case 1 is dominated by this monsoon-bridging requirement, not by nightly cycling.

When a second source is introduced (Cases 2, 3, or 4), the multi-day deficit can be served by generation rather than storage. The battery is then sized only for nightly cycling and short weather events, falling to 100 kWh. Adding a third source that is temporally complementary to the second (Case 5: wind plus biomass) allows the

battery to be sized only for the shortest-duration fluctuations, falling to 50 kWh. The 80% storage reduction of Case 5 is therefore the cumulative effect of two distinct substitutions: a multi-day deficit substitution from Case 1 to Case 2 (or Case 3, or Case 4), and a shoulder-hour substitution from those cases to Case 5. The mechanism is general; only the magnitudes are site-specific.

This view also explains why marginal benefit declines beyond two complementary sources. Once the multi-day and shoulder-hour deficits are both served by generation, further additions can only substitute for diurnal cycling, which is already small. The diminishing-returns shape of Fig. 3 is the empirical signature of this mechanism.

4.2. Comparison with published literature

The Case 5 LCOE of \$0.102/kWh sits at the lower end of the 0.05–0.15 \$/kWh range reported for multi-source rural HRES in published techno-economic studies [3, 4]. Earlier multi-source HRES case studies in India by [11] and similar analyses summarized by [7] report comparable LCOE values in the 0.10–0.21 \$/kWh band, consistent with the present results. The 80% battery reduction reported here is somewhat higher than the typical 60–70% range reported in those studies, which may reflect the favorable wind and biomass resource combination at the present case site. We do not interpret the higher reduction as a methodological advance but as a consequence of locally favorable resource complementarity.

The diesel-hybrid configuration (Case 2) reproduces the cost-savings pattern reported by [37] and others in the PV–diesel–BESS literature: 30–40% LCOE reduction relative to PV-only baselines, accompanied by direct emissions and fuel-price exposure. The present study confirms this pattern but extends the comparison to renewable-only alternatives that achieve similar cost savings without the emissions penalty.

Beluco et al. [22] formalized the complementarity-of-resources argument that underlies the hybridization benefit. A subsequent review Jurasz et al. [23] reviewed the empirical evidence for solar-wind complementarity at multiple geographic scales. The present results confirm both at the mini-grid scale and add biomass as a dispatchable third resource, reinforcing the empirical case for architecture-based design.

4.3. Cleaner production interpretation

The cleaner production framework defined by [32] and elaborated by [33] treats waste prevention at the design stage as the most effective intervention in the materials hierarchy. End-of-pipe mitigation, by contrast, accepts waste as inevitable and treats it. The hybridization mechanism described in Section 4.1 operates at the design stage: the choice of architecture determines the lifetime material intensity of the deployed system, before any material has been ordered. A 80% reduction in installed battery capacity translates to a proportional reduction in upstream demand for lithium, cobalt, and nickel, in transport-related emissions during installation, and in spent-battery volume at end of life. None of these reductions require subsequent recycling, recovery, or treatment infrastructure. They are achieved by not building the storage in the first place.

As an order-of-magnitude indication, under a representative lithium-ion battery pack material intensity of approximately 10 kg/kWh [14], the 200 kWh storage reduction achieved between Case 1 and Case 5 corresponds to roughly two tonnes of avoided battery hardware deployment per mini-grid-equivalent.

This is the cleaner production interpretation of the present results. Architecture-based design, applied at the planning stage of rural mini-grid projects, prevents storage-related material flows that would otherwise require management later. The framework is agnostic to the chemistry of the storage technology: a transition to alternative chemistries (sodium-ion, flow batteries, or solid- state) would shift the material profile but would not change the fact that less storage requires fewer materials. The cleaner production logic of the result is therefore robust to the storage-technology mix.

The cleaner production framing also clarifies why the diesel hybrid (Case 2) is excluded from the cleaner production solution space despite its competitive LCOE. Direct combustion emissions are end-of-pipe by definition, regardless of how cost-effective the configuration is on a levelized basis. Cases 3, 4, and 5 are the only configurations consistent with the cleaner production interpretation in the strict sense. Among these, Case 5 dominates on cost as well, eliminating the trade-off that the literature sometimes assumes between environmental performance and economic performance.

4.4. Cost–emission trade-off and the marginal cost of carbon avoidance

A useful summary metric is the marginal cost of carbon avoidance, computed as the LCOE premium of a renewable-only configuration over the diesel-hybrid Case 2, divided by the avoided emissions. For Cases 3 and 4, the marginal costs are \$0.008/kWh and \$0.0003/kWh respectively, both modest by comparison with typical carbon prices. For Case 5, the marginal cost is *negative* (\$–0.055/kWh): the configuration is both cheaper and cleaner than Case 2.

A negative marginal cost of carbon avoidance is uncommon in the literature, and we do not interpret it as a general property of multi-source hybrids. The negative value is also conditional on the diesel-hybrid (Case 2) being adopted as the comparator: if the comparator is shifted to the PV-only baseline (Case 1), the marginal cost becomes positive but small. It is the specific outcome of the favorable resource combination at the case site: simultaneous availability of sufficient solar irradiance, monsoon-aligned wind, and abundant agricultural biomass. At sites where one of these resources is absent or weak, the negative-cost outcome would not necessarily hold. The general finding is more cautious and more useful: at sites where two or more of these resources are available, the cost of the renewable-only solution is at most modestly above the fossil-hybrid solution, and may be below it.

4.5. Scope and limitations

The findings of the present study are bounded by assumptions that limit external validity. Three categories of limitation are relevant: modeling-framework limitations,

resource and cost-input uncertainties, and deployment-stage factors not modeled. Each is treated below in turn.

Modeling-framework limitations.. The HOMER Pro framework provides design-stage screening through hourly energy balance and lifecycle cost optimization. It does not capture sub-hourly dispatch dynamics, partial-load efficiency curves, transient response of inverters, control and protection coordination, or accelerated battery aging under specific cycling regimes. Wind turbine output is computed from vendor-specified power curves applied to extrapolated NASA POWER wind speeds, which may overstate field-measured capacity factors at low-wind inland sites [48, 49].

Resource and cost-input uncertainties.. NASA POWER, Global Solar Atlas, and NSRDB report slightly different annual GHI values for the study site, owing to differences in spatial resolution and processing methodology. The choice of database affects the absolute LCOE estimate but not the comparative ranking of configurations, which share the same solar resource input; the database-spread is in any case bounded by the GHI sensitivity range tested in Section 3.7. Component costs were approximated from representative market ranges reported in the literature and vendor quotations, with point values selected close to the median of each range. The cost ranking of configurations is robust within these ranges because the dominant cost drivers (PV array and lithium-ion battery) are explicitly tested in the sensitivity analysis. The cost vintage does not include technology learning curves; sustained price shifts, particularly for lithium-ion modules, would alter the absolute LCOE but not the relative ordering. Local biomass availability is site-specific and not transferable without local resource assessment.

Deployment-stage factors not modeled.. Several factors that affect real-world performance are outside the HOMER Pro lifecycle cost framework. These include control system complexity for multi-source architectures, operator skill requirements across multiple generation technologies, multi-vendor procurement and supply chain robustness, and institutional capacity for ongoing operation and maintenance. These factors generally favor simpler architectures in practice and may shift the deployment-stage optimum toward dual-source configurations (Cases 3 or 4) at sites with limited institutional capacity. Field-measured performance of small wind turbines at inland Indian sites has frequently fallen below predicted values, with reported capacity factors in the 8–15% range; vertical-axis wind turbines with cut-in speeds of 2–3 m/s offer a deployment-relevant alternative at low-wind sites and warrant pilot evaluation.

These factors do not invalidate the comparative finding within the modeled cost framework, but they constrain its interpretation. The results are best read as a design-stage screening that identifies attractive architectures and quantifies their relative performance under consistent assumptions, not as a detailed engineering specification of any single deployment. Detailed electrical modeling, full life-cycle assessment, and field validation through extended monitoring of an installed system are necessary before construction; these are identified as essential follow-on work in Section 5.

4.6. Practical implications for planners and DRE developers

The principal practical implication of these findings is that the question *which architecture?* is at least as important as the question *what component sizes?*, and probably more so for rural mini-grid projects with diverse local resource endowments. Component-centric procurement, in which a fixed PV-battery template is sized to fit local demand, leaves the storage savings of architecture diversification on the table. System-level planning, by contrast, begins with a resource inventory and selects the configuration tier that matches the inventory, before doing component sizing.

For Indian planners and decentralized renewable energy developers, this implies a two-stage workflow. First, screen candidate sites through a geographic-information-system overlay of solar, wind, biomass, and hydro resources to identify the feasible architecture tiers. Second, conduct site-specific optimization (HOMER Pro, etc) within the identified tier. The dimensionless indices introduced in this study (BCRI and ERI) provide a transferable language for reporting the outcomes of this two-stage process.

The findings also identify several enabling conditions that policy can address. Biomass supply chain reliability, addressed through state-level procurement frameworks and farmer-side incentive programs, would strengthen the feasibility of HRES architectures that include a gasifier. Capital subsidies for storage and for gasifier installation, accelerated depreciation, and net-metering arrangements that monetize surplus generation would each shift the configuration-level economics in favor of cleaner architectures. A detailed policy analysis is outside the scope of the present study but is identified as a natural direction for follow-on work.

5. Conclusions

This study evaluated progressive hybridization as a structural intervention for reducing battery storage in rural renewable mini-grids, through five HOMER Pro configurations on a calibrated 175 kWh/day case site. The main findings are:

1. **Storage is structurally reducible.** Battery capacity falls from 250 kWh to 50 kWh as resource diversity increases (BCRI = 0.80). Any single dispatchable or complementary addition delivers a uniform 60% reduction; the full multi-source hybrid achieves 80%.
2. **Cost and storage decline jointly.** Levelized cost decreases from \$0.236 to \$0.102 per kWh (INR 21.25 to INR 9.18, a 56.8% reduction) while reliability remains within LPSP $\leq$ 1%. The cost-optimal configuration is cost-competitive with current grid supply.
3. **Marginal benefit declines beyond two complementary sources.** Monsoon-bridging and shoulder-hour deficits are absorbed by the first two additions; subsequent diversification substitutes only for diurnal cycling.
4. **Hybridization aligns with cleaner production.** Reduced storage capacity translates proportionally to reduced upstream demand for lithium, cobalt, and

nickel. Architecture-based design therefore functions as design-stage pollution prevention.

5. **Framework transferable, magnitudes site-specific.** The BCRI, ERI, and stepwise hybridization methodology are independent of absolute load or cost. The reported magnitudes reflect the case site's resource endowment.

The stepwise hybridization framework and the proposed BCRI and ERI indices support comparative assessment of hybrid renewable mini-grid configurations in differing rural energy contexts. Four directions may extend the present work: (i) sub-hourly simulation to evaluate transient dispatch behavior and short-term variability; (ii) full life-cycle assessment of battery-intensive configurations; (iii) field validation by extended monitoring of an installed pilot system, including assessment of vertical-axis wind turbines for low-wind inland conditions; and (iv) integration of hydrogen storage and small hydropower within the hybridization framework. Together, these directions further place hybrid mini-grid design as both a system optimization problem and a pathway for reducing storage-related material burden.

CRediT authorship contribution statement

Asmelash Haftu Amaha: Conceptualization, Methodology, Software, Formal analysis, Investigation, Data curation, Writing – Original draft, Visualization. **Anand B. Rao:** Conceptualization, Methodology, Supervision, Writing – Review and editing, Project administration.

Declaration of competing interest

The authors declare that they have no known competing financial interests or personal relationships that could have appeared to influence the work reported in this paper.

Data availability

The data and HOMER Pro input files supporting the findings of this study are available from the corresponding author on reasonable request. An interactive dashboard is available at github.com/asmelash.github.io/, summarizing all five configurations.

Acknowledgments

The authors acknowledge Vigyan Ashram, Pabal, for site access and operational data, and the Centre for Technology Alternatives for Rural Areas (C-TARA), Indian Institute of Technology Bombay, for institutional support.

Declaration of generative AI use

The authors have used AI tools for language editing and improvement of clarity during the preparation of this manuscript. No AI tool was used to generate, fabricate, or misrepresent data or findings.

Nomenclature

Abbreviations

BCRI	Battery Capacity Reduction Index
BESS	Battery Energy Storage System
CAPEX	Capital Expenditure
CC	Cycle Charging (dispatch strategy)
CRF	Capital Recovery Factor
DG	Diesel Generator
ERI	Emission Reduction Index
GHI	Global Horizontal Irradiance
HOMER	Hybrid Optimization of Multiple Energy Resources
HRES	Hybrid Renewable Energy System
INR	Indian Rupee
IPCC	Intergovernmental Panel on Climate Change
LCOE	Levelized Cost of Energy
LF	Load Following (dispatch strategy)
LPSP	Loss of Power Supply Probability
MSEDCL	Maharashtra State Electricity Distribution Co. Ltd.
NPC	Net Present Cost
NSRDB	National Solar Radiation Database
O&M	Operation and Maintenance
OPEX	Operating Expenditure
PV	Photovoltaic
RF	Renewable Fraction
SoC	State of Charge
VAWT	Vertical-Axis Wind Turbine

Symbols

C_i	Battery capacity of configuration i (kWh)
C_{PV}	Battery capacity, PV-only baseline (kWh)
E_i	Annual emissions of configuration i (kg CO_2/yr)
E_{DG}	Annual emissions, diesel-hybrid baseline (kg CO_2/yr)
i	Real discount rate (%)
n	Project lifetime (years)

Units

\$	United States dollar
kW	Kilowatt
kWh	Kilowatt-hour
kWh/m^2/d	Daily solar irradiance
m/s	Wind speed
t/yr	Tonne per year (biomass)

Subscripts

i	Configuration index (Cases 1–5)
PV	Photovoltaic, baseline
DG	Diesel Generator, hybrid baseline

Bibliography

[1] International Energy Agency, Tracking SDG7: The Energy Progress Report 2024, Tech. rep., IEA, IRENA, UNSD, World Bank, WHO, Paris (2024).

[2] S. C. Bhattacharyya, D. Palit, Mini-grids for rural electrification of developing countries: Analysis and case studies from South Asia, Springer, 2014.

[3] S. Mandelli, J. Barbieri, R. Mereu, E. Colombo, Off-grid systems for rural electrification in developing countries: Definitions, classification and a comprehensive literature review, Renewable and Sustainable Energy Reviews 58 (2016) 1621–1646. doi:10.1016/j.rser.2015.12.338.

[4] F. F. Nerini, O. Broad, D. Mentis, M. Welsch, M. Bazilian, M. Howells, A cost comparison of technology approaches for improving access to electricity services, Energy 95 (2016) 255–265. doi:10.1016/j.energy.2015.11.068.

[5] F. Almeshqab, T. S. Ustun, Lessons learned from rural electrification initiatives in developing countries, Renewable and Sustainable Energy Reviews 82 (2018) 1982–1996. doi:10.1016/j.rser.2018.11.035.

[6] IRENA, Innovation outlook: Renewable mini-grids, Tech. rep., International Renewable Energy Agency (2016).

[7] P. K. Sharma, D. A. Kumar, P. William, D. Obulesu, P. M. Pandian, T. K. Khan, G. Manikandan, Energy storage system based on hybrid wind and photovoltaic technologies, Measurement: sensors 30 (2023) 100915.

[8] C. M. S. Kumar, S. Singh, M. K. Gupta, Y. M. Nimdeo, R. Raushan, A. V. Deorankar, T. A. Kumar, P. K. Rout, C. Chanotiya, V. D. Pakhale, et al., Solar energy: A promising renewable source for meeting energy demand in indian agriculture applications, Sustainable Energy Technologies and Assessments 55 (2023) 102905. doi:10.1016/j.seta.2022.102905.

[9] B. Bagheri, H. Kumagai, M. Hashimoto, M. Sugiyama, Techno-economic assessment of green hydrogen production in australia using off-grid hybrid resources of solar and wind, Energies 18 (13) (2025) 3285.

[10] C. P. Agupugo, A. O. Ajayi, C. Nwanevu, S. S. Oladipo, Policy and regulatory framework supporting renewable energy microgrids and energy storage systems, Eng. Sci. Technol. J 5 (2022) 2589–2615.

[11] S. Vendoti, M. Muralidhar, R. Kiranmayi, Techno-economic analysis of off-grid solar/wind/biogas/biomass/ fuel cell/battery system for electrification in a cluster of villages by HOMER software, Environment, Development and Sustainability 22 (2020) 351–372. doi:10.1007/s10668-019-00583-2.

[12] R. Kumar, H. K. Channi, A pv-biomass off-grid hybrid renewable energy system (hres) for rural electrification: Design, optimization and techno-economic-environmental analysis, Journal of cleaner production 349 (2022) 131347.

[13] C. A. Nallolla, V. Perumal, Optimal design of a hybrid off-grid renewable energy system using techno-economic and sensitivity analysis for a rural remote location, Sustainability 14 (22) (2022) 15393.

[14] IRENA, Renewable power generation costs in 2023 – battery trends and economics, Tech. rep., International Renewable Energy Agency (2024).

[15] R. Tarife, Y. Nakanishi, Y. Chen, Y. Zhou, N. Estoperez, A. Tahud, Optimization of hybrid renewable energy microgrid for off-grid rural agriculture in camiguin island, philippines, Energies 15 (6) (2022) 2251.

[16] J. Liu, Z. Wang, Y. Zhang, Hybrid renewable energy applications in zero-energy communities with stationary battery and mobile hydrogen vehicle storage, Energy 214 (2021) 118858. doi:10.1016/j.energy.2020.118858.

[17] S. Anvari, A. Fatima, R. Chauhan, Sustainable solar/biomass/energy storage hybridization for off-grid rural mini-grids, Renewable and Sustainable Energy ReviewsIn press (2025).

[18] S. Anvari, A. Medina, R. P. Merchán, A. C. Hernández, Sustainable solar/biomass/energy storage hybridization for enhanced renewable energy integration in multi-generation systems: A comprehensive review, Renewable and Sustainable Energy Reviews 223 (2025) 115997.

[19] Z. J. Zhu, N. Espinosa, S. M. Jordaan, Life cycle assessment of solar photovoltaic–battery systems: A canadian case study, Sustainable Energy Technologies and Assessments 90 (2026) 105017. doi:10.1016/j.seta.2026.105017.

[20] L. Li, B. Wang, K. Jiao, M. Ni, Q. Du, Y. Liu, B. Li, G. Ling, C. Wang, Comparative techno-economic analysis of large-scale renewable energy storage technologies, Energy and AI 14 (2023) 100282. doi:10.1016/j.egyai.2023.100282.

[21] S. Algarni, V. Tirth, T. Alqahtani, S. Alshehery, P. Kshirsagar, Contribution of renewable energy sources to the environmental impacts and economic benefits for sustainable development, Sustainable energy technologies and assessments 56 (2023) 103098. doi:10.1016/j.seta.2023.103098.

[22] A. Beluco, P. K. Souza, A. Krenzinger, A dimensionless index evaluating the time complementarity between solar and hydraulic energies, Renewable Energy 33 (10) (2008) 2157–2165.

[23] J. Jurasz, F. A. Canales, A. Kies, M. Guezgouz, A. Beluco, A review on the complementarity of renewable energy sources: Concept, metrics, application and future research directions, Solar Energy 195 (2020) 703–724. doi:10.1016/j.solener.2019.11.087.

[24] P. Roy, J. He, T. Zhao, Y. V. Singh, Recent advances of wind-solar hybrid renewable energy systems for power generation: A review, IEEE Open Journal of the Industrial Electronics Society 3 (2022) 81–104.

[25] Y. Sawle, S. Gupta, A. Kumar Bohre, Pv-wind hybrid system: A review with case study, Cogent Engineering 3 (1) (2016) 1189305.

[26] M. F. Ali, M. M. Rahman, M. E. Chowdhury, Techno-economic and predictive modeling of a solar pv–biogas system for residential supply, IEEE AccessOnline (2025).

[27] M. R. B. Khan, R. Jidin, J. Pasupuleti, S. A. Shaaya, Optimal combination of solar, wind, micro-hydro and diesel systems based on actual seasonal load profiles for a resort island in the south china sea, Energy 82 (2015) 80–97.

[28] D. Biswas, M. F. Ali, M. Saha, M. S. Alam, M. Ali, M. A. AlAqil, O. Obaidi, M. K. Islam, Techno-economic optimization, sensitivity analysis and stability evaluation of a high-renewable hybrid microgrid for rural bangladesh, Scientific Reports (2026).

[29] Y. Kalinci, A. Hepbasli, I. Dincer, Life cycle assessment of hydrogen production from biomass gasification systems, International Journal of Hydrogen Energy 37 (19) (2012) 14026–14039.

[30] X. Zhang, G. Ma, W. Huang, S. Chen, S. Zhang, Short-term optimal operation of a wind-pv-hydro complementary installation: Yalong river, sichuan province, china, Energies 11 (4) (2018) 868.

[31] Q. Hassan, S. Algburi, A. Z. Sameen, H. M. Salman, M. Jaszczur, A review of hybrid renewable energy systems: Solar and wind-powered solutions: Challenges, opportunities, and policy implications, Results in Engineering 20 (2024) 101621. doi:10.1016/j.rineng.2023.101621.

[32] M. Geissdoerfer, P. Savaget, N. M. P. Bocken, E. J. Hultink, The Circular Economy: A new sustainability paradigm?, Journal of Cleaner Production 143 (2017) 757–768.

[33] P. Ghisellini, C. Cialani, S. Ulgiati, A review on circular economy: the expected transition to a balanced interplay of environmental and economic systems, Journal of Cleaner Production 114 (2016) 11–32.

[34] C. A. John, L. S. Tan, J. Tan, P. L. Kiew, A. M. Shariff, H. N. Abdul Halim, Selection of renewable energy in rural area via life cycle assessment-analytical hierarchy process (lca-ahp): A case study of tatau, sarawak, Sustainability 13 (21) (2021) 11880.

[35] J. F. Manwell, J. G. McGowan, A. L. Rogers, Wind Energy Explained: Theory, Design and Application, 2nd Edition, John Wiley and Sons, Chichester, UK, 2009. doi:10.1002/9781119994367.

[36] N. N. Davis, J. Badger, A. N. Hahmann, B. O. Hansen, N. G. Mortensen, M. Kelly, X. G. Larsén, B. T. Olsen, R. Floors, G. Lizcano, P. Casso, O. Lacave, A. Bosch, I. Bauwens, O. J. Knight, A. P. van Loon, R. Fox, T. Parvanyan, S. B. K. Hansen, D. Heathfield, M. Onninen, R. Drummond, The Global Wind Atlas: A high-resolution dataset of climatologies and associated web-based application, Bulletin of the American Meteorological Society 104 (8) (2023) E1507–E1525. doi:10.1175/BAMS-D-21-0075.1.

[37] A. Aziz, M. F. N. Tajuddin, M. Adzman, M. Ramli, S. Mekhilef, Energy management and optimisation of pv/diesel/battery hybrid energy systems using combined dispatch strategy, Energy Conversion and Management (2019).

[38] V. Salas, M. Alonso-Abella, F. Chenlo, E. Olías, Analysis of the maximum power point tracking in the photovoltaic grid inverters of 5 kw, Renewable Energy 34 (11) (2009) 2366–2372.

[39] D. Tsuanyo, Y. Azoumah, D. Aussel, P. Neveu, Modeling and optimization of batteryless hybrid PV (photovoltaic)/diesel systems for off-grid applications, Energy 86 (2015) 152–163.

[40] G. Glenk, S. Reichelstein, Economics of converting renewable power to hydrogen, Nature Energy (2019).

[41] D. Parra, M. Gillott, S. A. Norman, G. S. Walker, Optimum community energy storage system for PV energy time-shift, Applied Energy 137 (2015) 576–587.

[42] T. Lambert, P. Gilman, P. Lilienthal, Micropower system modeling with homer, Integration of Alternative Sources of Energy (2006) 379–418doi:10.1002/0471755621.ch15.

[43] HOMER Energy LLC, HOMER Pro: Hybrid optimisation of multiple energy resources, version 3.15, Software, hOMER Energy LLC, Boulder, CO, USA (2023). URL https://www.homerenergy.com/products/pro/

[44] V. Suresh, M. Muralidhar, R. Kiranmayi, Modelling and optimization of an off-grid hybrid renewable energy system for electrification in a rural areas, Energy Reports 6 (2020) 594–604. doi:10.1016/j.egyr.2020.01.013.

[45] F. Antonanzas-Torres, J. Antonanzas, J. Blanco-Fernandez, State-of-the-art of mini grids for rural electrification in west africa, Energies 14 (2021) 990.

[46] C. Mao, M. Wood, L. David, S. J. An, Y. Sheng, Z. Du, H. M. Meyer, R. E. Ruther, D. L. Wood, Selecting the best graphite for long-life, high-energy Li-Ion batteries, Journal of The Electrochemical Society 165 (9) (2018) A1837–A1845. doi:10.1149/2.1111809jes.

[47] IPCC, Climate change 2021: The physical science basis. contribution of Working Group I to the Sixth Assessment Report, Tech. rep., Intergovernmental Panel on Climate Change, Cambridge, U.K. (2021).

[48] S. Sinha, S. Chandel, Review of software tools for hybrid renewable systems, Renewable and Sustainable Energy Reviews (2014). doi:10.1016/j.rser.2014.01.035.

[49] S. Sinha, S. Chandel, Review of recent trends in optimization techniques for solar photovoltaic–wind based hybrid energy systems, Renewable and Sustainable Energy Reviews 50 (2015) 755–769. doi:10.1016/j.rser.2015.05.040.